

Design and Analysis of MEMS-Based Piezoresistive Accelerometer with Low Cross-Axis Sensitivity

Tapas Kumar Mohanty¹ V.S. Krushnasamy²

¹ PG Student Department of Instrumentation and Control Engineering SRM University Chennai, Tamil Nadu

² Asst. Professor Department of Instrumentation and Control Engineering SRM University Chennai, Tamil Nadu

Abstract: This paper presents a design and development of a high-performance silicon piezoresistive MEMS accelerometer, with a finite element analysis (FEA) and low cross-axis sensitivity. Finite element analysis is used to simulate electro statically actuated piezoresistive accelerometer operating under dc conditions .The designs presented in this paper consist of a square shaped proof mass with flexures supporting it. Due to of the opposite nature of stress at two ends, these piezoresistors can be connected to form a Wheatstone bridge so that the cross-axis responses are practically reduced .The piezoresistors are placed near the proof mass and frame ends on the flexure. The simulations show the von Misses stress, displacement, Eigen frequency plot, voltage distribution and temperature change in the piezoresistors using COMSOL 4.3 Multiphysics.

Keywords: Single Silicon piezoresistive accelerometer, MEMS, Wheatstone bridge

I. INTRODUCTION

Since with change of time, MEMS technology has undergone rapid development, leading to the successful fabrication of miniaturized mechanical structures integrated with microelectronic components. Initially the accelerometers designed were based on the principle of electro magnetism which were large bulky and costly. MEMS technology has been able to optimize the size and cost issues involved in the design of accelerometers [1, 2]. Large number of accelerometers has been designed till now based on Capacitive, Piezoelectric and Piezoresistive type. This paper focuses on the design process leading to a typical MEMS device a piezoresistive accelerometer. Accelerometers are in greatly useful for specific applications ranging from guidance and stabilization of space-crafts, measure tilt motion, vibration and high shock application. Generally, it is desirable that accelerometers exhibit a linear response and a high signal-to-noise ratio, simple in structure easy to fabricate and easily affected by electromagnetic capacitance. Among the many technological alternatives available, piezoresistive accelerometers are manifest. They suffer from dependence on temperature and low resolution, but have a DC response, simple readout circuits, and are capable of high sensitivity and reliability. In addition, it is a low-cost technology suitable for high-volume production [3]. So that the accelerometer can measure very high acceleration is because it has a very large proof mass. Therefore the designs in this paper have been made for applications in to measure high acceleration of spacecraft or aircraft motion.

II. DEVICE CONFIGURATION

The two configurations of accelerometers are shown in fig 1. The structure consists of silicon (100) substrate consisting of flexures, proof mass and four supporting frame. The p-type single crystal silicon (110) piezoresistors are placed along on the substrate. The proof mass is supported via these flexures. On each flexure, two piezoresistors are placed at maximum stress locations, one near the proof mass and other near the frame. The accelerometer was designed to sense acceleration up to 20g with low off axis sensitivity. The dimensions of various parts of accelerometer structure are as follows:

- Proof mass 3500 μ m (L)*3500 μ m (W)*300 μ m (h).
- Flexures 1200 μ m (L)*250 μ m (W)*35 μ m (h).
- Frames 6000 μ m (L)*200 μ m (W)*250 μ m (h).
- Piezoresistors 100 μ m (L)*20 μ m (W)*2 μ m (h).



Fig 1: Configurations

III. DESIGN AND PRINCIPLE OF PIEZO-RESISTIVE ACCELEROMETER

The first MEMS-based Accelerometer was proposed by Roy lance and Angell (1979). This design contains a proof mass attached to silicon through a short flexural element. The implantation of a piezoresistive material on the upper surface of the flexural element was used for measuring out-of-plane acceleration of the proof mass. The accelerometer behaves as a damped mass on a spring. When the accelerometer experiences acceleration the mass is displaced and the displaced is then measured to give the acceleration. These techniques are commonly used to convert mechanical motion into an electrical signal.

1.1 Design Model and Analysis

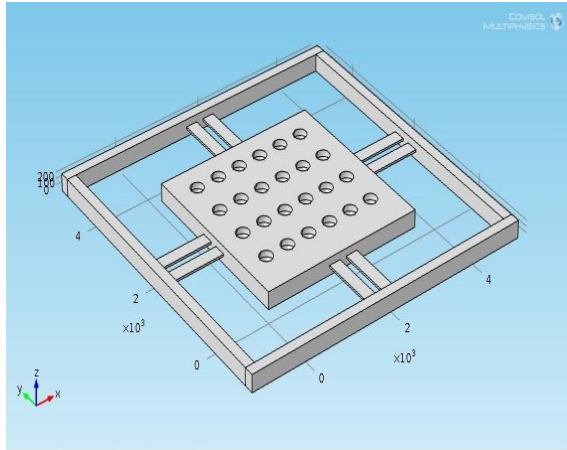


Fig 2: 8 flexures

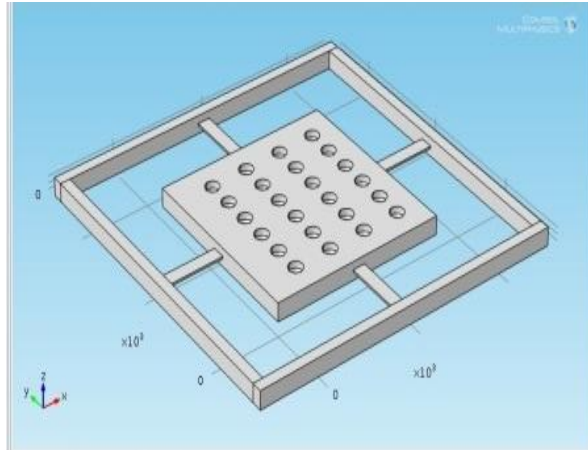


Fig 3: 4 flexures

3.2 Stress Analysis

The structures designed in the paper can be modelled as a beam fixed [4] at both ends with a point load in the centre for stress analysis. So 20g force is applied on the top surface of the proof-mass in the opposite of Z-direction. The force has to be founded by the product of volume of proof mass with density of the materials along the top surface of the proof mass.

By equation 1 we found the maximum displacement and by equation 2 we found the maximum stress

$$\delta(x) = \frac{Fx^2}{6EI} (3L - x) \tag{1}$$

Where, x is the distance from the support that stress is applied.

Maximum stress

$$\text{Stress } (\sigma) = \frac{F}{A} \tag{2}$$

Where, F = Applied Force (equal to 20g)

A = Cross-sectional area of the proof mass of the accelerometer.

The von misses stress and displacement in the two configurations show the similarity with the result obtained in simulation shown in Fig 5 and Fig 6

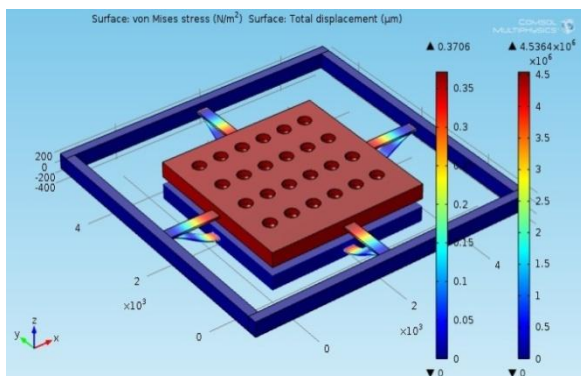


Fig 4: Simulation of 4 flexures accelerometer

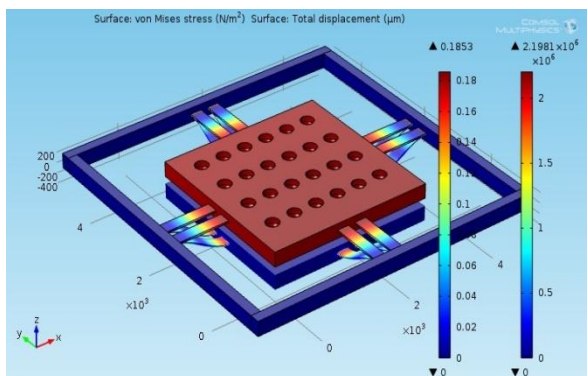


Fig 5: Simulation of 8 flexures accelerometer

3.3 Stress free Resistance

The resistance of the piezoresistor is given by $R = \rho L_0/A$, where L_0 is the length and A the cross-section area. Assuming that the stress is applied in the longitudinal direction the change in resistance ΔR is given by [11]

$$\frac{\Delta R}{R_0} = \pi_1 \sigma_1 \tag{3}$$

Where R_0 is the initial resistance, π_1 is the longitudinal piezoresistive coefficient and σ_1 the longitudinal stress. The piezoresistive coefficients are dependent on the dopant concentration, crystal orientation and temperature. For both p- and n-type silicon, the value of the piezoresistive coefficient decreases with increasing temperature and doping concentrations. The values π_{11}, π_{12} and π_{44} of and for single-crystalline silicon under certain doping concentration and dopant types have been experimentally characterized.

If the piezoresistors (110) are aligned along the silicon crystal (100) the piezoresistive coefficient is

$$\pi_1[110] = \frac{1}{2} [\pi_{11} + \pi_{12} + \pi_{44}] \tag{4}$$

The piezoresistive coefficient can be written as a function of dopant concentration, N and temperature T as $\pi_1(N, T) = P(N, T)\pi_1(300K)$, where $P(N, T)$ is the piezoresistive factor and $\pi_1(300K)$ [8] is the piezoresistive coefficient at room temperature. The piezoresistive factor is almost independent of the dopant concentration for impurity level lower than 10^{18} cm^{-3} . So the piezoresistive coefficient can be expressed as

$$\pi_1(T) = P(T)\pi_1(300K). \tag{5}$$

The piezoresistive coefficient along the (110) direction in the single-crystal silicon is $\pi_{1(110)}(300K) = 71.8 \cdot 10^{-11} \text{ pa}^{-1}$ by using the equation 2. For lower resistivities, the piezoresistive coefficient and the sensitivity of the sensor is highly decreased.

Several typical values for selected doping concentrations are listed in Table 1.

Table 1: Piezo-resistivity Components for Single-Crystal silicon under certain Doping values

Piezo-resistance Co-efficient (10^{-11} pa^{-1})	n-type (resistivity = 11.7 Ω -cm)	p-type (resistivity = 7.8 Ω -cm)
π_{11}	-102.2	6.6
π_{12}	53.4	-1.1
π_{44}	-13.6	138.1

3.4 Piezoresistor positioning (Cross-off axis analysis)

The change in the resistivity of a piezoresistive material is directly proportional to the stress, so it is very important to place these resistors at the maximum stress points to get higher sensitivity. The accelerometers are designed to measure acceleration only in Z-axis with low-off axis along X or Y-axis. The piezoresistors are connected to form a Wheatstone bridge configuration for acceleration detection in fig 7 and the resistors are connected in such a direction that bridge should be at balanced condition during X-axis and Y-axis direction. The resistors at the proof mass end can identify by R_m and the frame denotes by R_f .

From stress analysis, it would be found that the stress on two ends of the supporting beam is opposite in nature. By applying 20g along Z-direction it shows the first stress peak which occurs near the frame end which is tensile in nature whereas the second stress peak near the mass end which is compressive in nature. These stress peaks define the favourable positions where the piezoresistors must be placed to get higher sensitivity. Since the piezoresistors have transverse placement on the beam, their resistance increases under compressive stress and decreases under tensile stress. Finally we got zero cross-off by using bridge. In response to differential acceleration, change of accelerometer output voltage is given by [9]

$$\Delta V = \frac{\Delta R}{R} V_b \tag{6}$$

Where, V_b is the wheat stone bridge supply voltage, ΔR is the change of resistance of the piezoresistor and R is the initial resistance.

The equation 3 is written as [11]

$$\frac{\Delta R}{R_0} = G \frac{\Delta L}{L_0} \tag{7}$$

Where L_0 is the initial length of a piezoresistor

ΔL is the change in length due to applied acceleration

G gauge factor= 120.6 found from calculation ($G=E_1\pi_1$)

E_1 Young's modulus = 169GPa

The accelerometer is configured as a wheat stone half bridge, and then the relationship between the input voltage and output voltage is

$$\frac{V_{out}}{V_{in}} = \frac{\Delta R}{R_0} \tag{8}$$

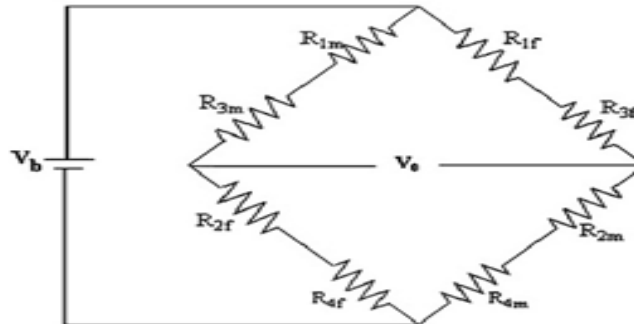


Fig 7: wheat stone bridge circuit

Table 2. Effect of acceleration along different axes on piezoresistor.

Piezoresistors	ΔR for X-axis (direction)	ΔR for Y-axis (direction)	ΔR for Z-axis (direction)
R_{1m}	Downward	Downward	Downward
R_{1f}	Upward	Upward	Upward
R_{2m}	Upward	Downward	Downward
R_{2f}	Downward	Upward	Upward
R_{3m}	Upward	Upward	Downward
R_{3f}	Downward	Downward	Upward
R_{4m}	Downward	Upward	Downward
R_{4f}	Upward	Downward	Upward

3.5 Sensitivity Analysis

Sensitivity is determined from the stiffness constant and the effective mass of the accelerometer. The resonant frequency is also determined from the effective stiffness constant and the effective mass [6]. The relationship between sensitivity and resonant frequency with effective mass and stiffness constant.

$$\text{Sensitivity (S)} = \frac{\text{output voltage}}{\text{acceleration}} = \frac{V_{out}}{a} \tag{9}$$

It also defined as relative change of output per applied differential acceleration

$$S = \frac{\Delta V}{\Delta g} \frac{1}{V_b} = \frac{\Delta R}{R} \frac{1}{\Delta g} \tag{10}$$

From FEA resistivity change of the accelerometer was found 0.4% for 20g in Z-axis which is on 2.357K Ω piezoresistor which is little bit large compared in the paper [4].

The acceleration of the accelerometer is calculated by

$$a = \omega_n^2 x = \frac{kx}{m} \tag{11}$$

Where ω_n the natural frequency (radian s^{-1}), m is the mass of proof-mass, and x is the deflection of the centre of the proof mass. K is the stiffness constant, $K = F/\delta$ found for the proof mass is 4.218×10^{-3} as mass = 7.919×10^{-7} kg and force (F) = 1.5664×10^{-3} N for 20g acceleration. The natural frequency also calculated as

$$f_n = \frac{1}{2\pi} \sqrt{\frac{k}{m}} = 3.656 \text{ KHz for the accelerometer.}$$

IV. RESULTS

Due to the acceleration applied on the accelerometer the variation of the stress of the proof mass shown in the fig 8. The accelerometer 1 defined 4 flexures accelerometer and 2 defined the 8 flexures accelerometer.

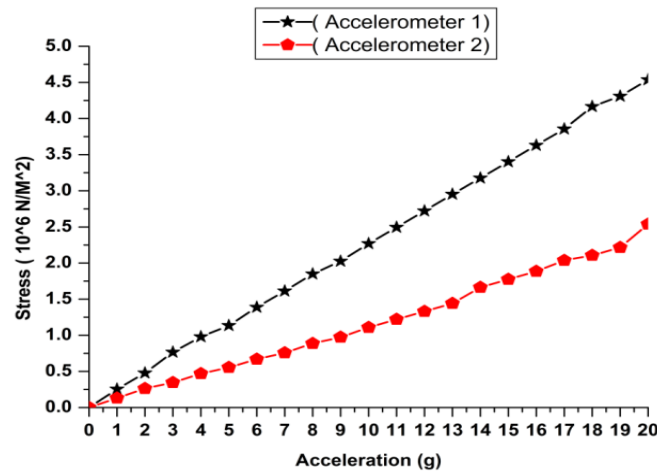


Fig 8: Variation of accelerometer stress with Z-axis acceleration.

By providing supply voltage 12V and applied differential acceleration the acceleration output shown in fig 9

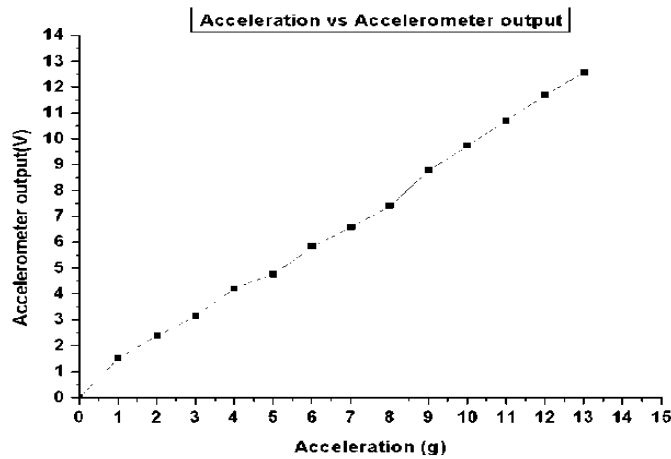


Fig 9: Variation of wheat stone output with different acceleration

By changing the room temperature the variation of stress of accelerometer can be analysed in fig 10

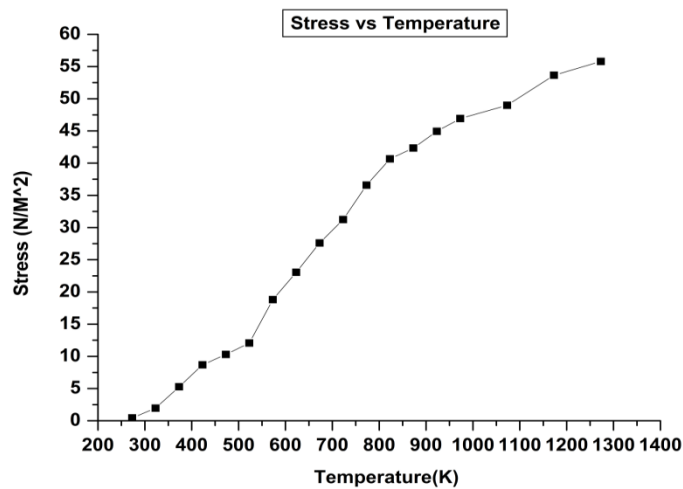


Fig 10: variation of stress due to change in room temperature.

Piezoresistor acceleration along X, Y and Z axis, due to different Eigen frequency is shown in fig 11

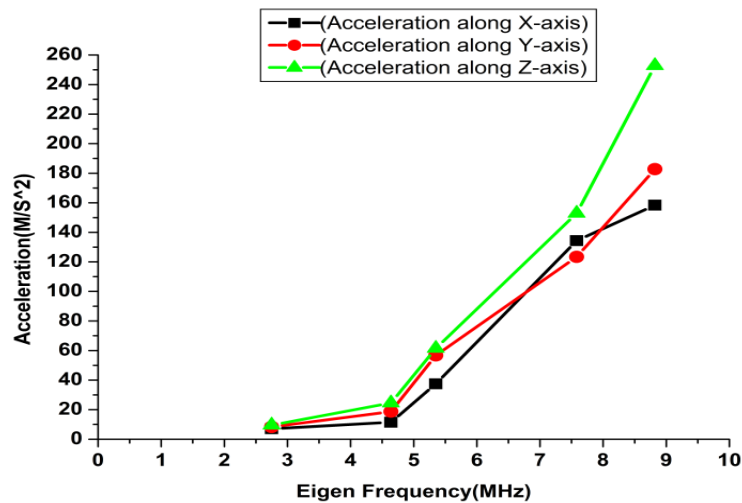


Fig 11: Variation of acceleration with Eigen frequency

V. CONCLUSIONS

A fully completed study for the design and analysis of MEMS based Piezoresistor accelerometer with low cross-axis sensitivity has been simulated in this paper. Mechanical configuration of the sensor is designed to reduce the structural asymmetry along the device. The direction which improves the device stability by decreasing the difference between the center of proof mass and the flexures. Simulations reveal that these structures would have high shock survivability therefore in addition to aircraft motion sensing such structures can be used to measure high gravity .[12] Piezoresistors can be defined as single mask technique [5].

REFERENCES

- [1]. L.C. Spangler and C.J. Kemp, "Integrated silicon automotive accelerometer," *Sens. Actuators*, A54, pp. 523–529, 1996.
- [2]. T. Velten, P. Krause, and E. Obermeier, "Two-axis micromachined accelerometer for Gesture Recognition," *MME*, 1996, pp. 247–250.
- [3]. Garcia-Valenzuela and M. Tabib-Azar, "Comparative study of piezoelectric, piezoresistive, electrostatic, magnetic, and optical sensors," *Proc. SPIE*, 1994, pp. 125–142.
- [4]. A. Chaehoi, L. Latorre, P. Nouet, and S. Baglio, "Piezoresistive CMOS Beams for Inertial Sensing," *Proceedings of IEEE Sensors*, Toronto, pp. 451, 2003.
- [5]. N. Yazadi, K. Najafi, A.S. Salián, A. High-Sensitivity, accelerometer with a folded-electrode structure, *J. Microelectromech. Syst.* 12 (2003) 479–486.
- [6]. K. Kwon, S. Park, A Bulk, Micromachined three-axis accelerometer using silicon direct bonding technology and polysilicon layer, *Sens. Actuators A* 66 (1998) 250–255.
- [7]. M.K. Lim, H. Du, C. Su, W.L. Jin, A micromachined piezoresistive accelerometer with high sensitivity: design and modelling, *Microelectronic Engineering* 66 (1999) 263–272.
- [8]. Kanda Y 1982 A graphical representation of the piezoresistive coefficient in silicon *IEEE Trans. Electron Devices* 30 802-10.
- [9]. K. Okada, Tri-axial piezoelectric accelerometer, Tech. Digest, 8th Int. Conf. Solid-state Sensors and Actuators (Transducers '95/Eurosensors IX), Stockholm, Sweden, 25–29 June, 1 (1995) 554–557.
- [10]. M.K. Lim, H. Du, C. Su, W.L. Jin, A micromachined piezoresistive accelerometer with high sensitivity: design and modelling, *Microelectronic Engineering* 66 (1999) 263–272.
- [11]. Kanda Y 1991 Piezoresistance effect of silicon *Sensors Actuators A* 28 83-91.
- [12]. Mohd Haris and Hongwei Qu, "A CMOS-MEMS Piezoresistive Accelerometer with Large Proof Mass", *Proceedings of the 2010 5th IEEE conference on Nano/Micro Engineered and Molecular Systems*, Xiamen-China, pp. 309, 2010.